



Article

Non-Newtonian Nano-Fluids in Blasius and Sakiadis Flows Influenced by Magnetic Field

Imran Abbas ^{1,†}, Shahid Hasnain ^{2,†}, Nawal A. Alatawi ^{2,†}, Muhammad Saqib ^{3,†} and Daoud S. Mashat ^{2,*}¹ Department of Mathematics, Faculty of Science, Air University, Islamabad Campus 44000, Pakistan² Department of Mathematics, Faculty of Science, King Abdulaziz University, Jeddah 21589, Saudi Arabia³ Department of Mathematics, Khwaja Fareed University of Engineering & Information Technology, Rahim Yaar Khan 48800, Pakistan

* Correspondence: dmashat@kau.edu.sa

† These authors contributed equally to this work.

Abstract: Current study solves heat transfer and fluid flow problem in Newtonian and non-Newtonian nano-fluids through a permeable surface with a magnetic field effects which is done in the presence of injection and suction for the first time. In order to solve the governing partial differential equations numerically, we used the Runge-Kutta Fehlberg (RKF45) technique in which the similarity transformation method is applied. This approach converts the governing partial differential equations into ordinary differential equations. In this particular investigation nano-particles of copper, copper oxide, titanium dioxide, and aluminium oxide are studied by considering CMC/water as a base fluid with the effect of magnetic field on the classical Blasius and Sakiadis flows of nano-fluids. Validation is carried out using the previously obtained numerical findings. We looked at the power-law index (n), the volume fraction (φ) of nano-particles and the permeability parameter (f_w) which affects the flow of nano-fluid and the transfer of heat. Non-Newtonian nano-fluid demonstrates superior performance in terms of heat transfer when compared to Newtonian nano-fluid in both the injection and the impermeable surfaces. Altering the nano-particles' composition, on the other hand, has a far greater impact on the heat transfer process that occurs during suction. Graphics show the impacts of governing physical parameters on Blasius and Sakiadis flow velocity, temperature, skin friction coefficient, and reduced Nusselt number. Physical and engineering interest are explored in detail.

Keywords: Newtonian & non-Newtonian nano-fluids; permeable surface; suction & injection; Sakiadis & Blasius flows; similarity transformation; Runge-Kutta Fehlberg (RKF45)



Citation: Abbas, I.; Hasnain, S.; Alatawi, N.A.; Saqib, M.; Mashat, D.S. Non-Newtonian Nano-Fluids in Blasius and Sakiadis Flows Influenced by Magnetic Field.

Nanomaterials **2022**, *12*, 4254. <https://doi.org/10.3390/nano12234254>

Academic Editor: Henrich Frielinghaus

Received: 30 September 2022

Accepted: 23 November 2022

Published: 29 November 2022

Publisher's Note: MDPI stays neutral with regard to jurisdictional claims in published maps and institutional affiliations.



Copyright: © 2022 by the authors. Licensee MDPI, Basel, Switzerland. This article is an open access article distributed under the terms and conditions of the Creative Commons Attribution (CC BY) license (<https://creativecommons.org/licenses/by/4.0/>).

1. Introduction

Non-Newtonian fluids have been the focus of study on drag force and energy transfer over the last half century. This is because, the widespread usage trend of applications using Non-Newtonian and Newtonian fluids within the manufacturing sector, such as molten polymers, slurries, pulps and emulsions. The increasing demands of contemporary technologies, in the realms of petrochemicals, electricity generation, and microelectronics need to create more efficient fluids of different sorts for according to the efficiency of the heat transfer. Nano-fluids are made by dispersing solid particles on the nano-scale scale into low viscosity base liquids such as water, ethylene glycol (EG), and oils all have high heat conductivity. Therefore, it has become difficult to find appropriate nano-fluids with enhanced heat transfer capabilities and high thermal conductivity. Thermal conductivity of oxide nano-fluids has been the subject of several published investigations such as, Cu , TiO_2 , SiO_2 and Al_2O_3 . In these investigations, a research on the relationship between solid content and thermal conductivity was carried out. Nano-particles enhance fluids thermal conductivity significantly, which in turn improves the heat transfer properties. Therefore, dispersing micro/nano sized particle materials in liquid boosts the thermal conductivity of the fluids. Viscosity increment is due to addition of nano-particles which reduces the

thermal advantages of nano-fluids by necessitating more pumping power in the systems. Nano-fluids' thermal behaviour is one of the most essential issues, however the most important problem is the stability of the nano-fluids which is still difficult to achieve the appropriate level of stability in today's world. Although reducing the concentration of nano-fluids is the best method to preserve excellent fluidity, most studies have instead concentrated on the suspension stability of nano-fluids with no significant outcomes. Non-Newtonian fluids give platform to describe the rheological characteristics of nano-fluids by the constitutive equations which are based on empirical or semi-empirical formulae. In addition, the non-linear terms of the associated differential systems are increased by the presence of additional rheological factors in such interactions. To this end, the literature presents a wide variety of non-Newtonian fluid models (each with its own unique rheological effects) [1–6].

Sui et al. [7] studied the use of power law model for non-Newtonian fluids with boundary layer (BL) using mixed convection mechanism to get insights about heat transfer. A moving conveyor along an inclined plate was proposed by them, using the homotopy analysis (HAM) technique, they conducted in depth the numerical simulations of the temperature profile and the effects of power-law viscosity and shear flow. Numerical study of the heat transfer using fluids with shear thickening behaviour on permeable stretching plane which give rise to BL flow, done by Jalil et al. [8]. They founded accurate analytical and numerical solutions to the similarity equations in non-linear case of study. The numerical investigation done by Ahmed et al. [9] along with boundary layer theory, by using power law fluid which placed on stretched sheet for fluid flow and transfer of heat. In order to get analytical and numerical solutions to the proposed equations, they made use of the homotopy (HAM) technique coupled with shooting method. Guha et al. [10] took into consideration free convection boundary layer flow as part of their investigation. The finite difference time marching method was the approach which used to solve the problem. Meghdad et al. [11] considered fluid with power law nature over flat vertical surface in case of two dimensional problem for fluid flow and transfer of heat. They proposed, a non-linear stretching of the surface which was coupled with consideration of heat radiation, to investigate the influence of buoyancy parameter on mixed convection. Fluid which pass over a porous and flat plate, considered by Kishan et al. [12] to solve BL problem with help of finite difference (FD) schemes while same group carried out the numerical analysis to power law fluid by considering convection with mixed nature. A power law fluid along the impact of magnetic field, effect of radiation, heat generation/absorption and thermal dispersion on permeable flat and stretched plates, with viscous dissipation effects are studied to investigate heat transfer and fluid flow problem [13,14].

Ram Reddy et al. [15] considered porous medium or non-darcy material to performed a computational simulation for a sloping, inclined plate. A study of a power law non-Newtonian fluid flowing over a moving surface on surface slip and heat absorption or generation in heat transfer and fluid flow. Such researched heat transport in non-Newtonian, non-uniform fluids. A slip boundary layer and viscous dissipation at a specific permeable surface employing power law fluid is analysed. Temperature drop and velocity slip in a pseudo-plastic fluid moving across a porous surface in a magnetic field are observed [16–19]. Although many articles have been written about the fluid flow and the heat transfer due to non-Newtonian fluids over variant surfaces (permeable) which devoid of nano-particles because their authors were unaware of the existence of the newer field of study. Choi invented the term nano-fluid to describe a novel class of heat transfer fluids made by floating metallic nano-particles in ordinary fluids. When base fluids are compared with other nano-fluids for heat transfer indicate the improvement in thermal conductivity and convective heat transfer [20–28]. Water, ethylene glycol, oil, and other heat transfer fluids are used as base fluids. Nano-particles are made from metallic (like copper), metal oxide, carbon-based, or combinations of these elements [29–35]. Non-Newtonian nano-fluids with assumption of Brownian motion during the simulation of flow, mass, and heat transfer which included a transverse magnetic field, injection, and suction over a

permeable stretched sheet, investigated by Sandeep et al. [36]. Non-Newtonian nano-fluids flow over stretching sheet with non-linear properties which was subject of research of Madhu et al. [37]. The non-Newtonian behaviours and heat transfer brought about by the introduction of a magnetic field are the primary topic that are covered in this article. Therefore, a literature concentrated on certain fields and applications is viewable from inside the literature [38–43].

Nano-fluids flow over horizontal plate with Sakiadis and Blasius effects, are the focus of all of the investigations that have been discussed so far. However, as of yet, no contribution has been made on non-Newtonian (NN) nano-fluids (NFs) considering magnetic field over surface which is a porous, because of the nano-particles that consist of *Cu*, *CuO*, *TiO₂*, and *Al₂O₃*. Therefore, the mixture of sodium carboxymethyl cellulose (CMC) and water used as a base fluid for current research. In Sakiadis and Blasius flows, energy, continuity and momentum equations are governing system which is the main focus of this work. The use of an appropriate similarity transformation and then solved numerically through MATLAB. In the next section, we explore further into the formation patterns with physical and rheological features of nano-fluids along the mathematical formulation and method of solution and discussion.

1.1. Rheological and Thermal Characteristics of Nano-Fluids

Solids dispersed in liquids enhance heat conductivity, since from 1900s, scientists and engineers have added solid particles to liquids to increase their low heat conductivity. The increment in thermal conductivity of solid-dispersed liquids in which size of particles was restricted to microns or millimetres and solid particle concentration was predicted by Maxwell and Yang [44–46]. Over the past decades, several organisations and corporations have studied nano-fluids for their potential to improve heat transfer coefficients. The traditional Maxwell theory or the H-C [35] model did not predict the thermal conductivity anomaly. Many hypothesised processes explain nano-fluids' heat transfer phenomena however, these models were inconsistent and limiting in scope, until Maxwell proposition which was proposed in 19th century about suspension thermal conductivity [46]. Such model reveals that the solid-liquid combination has better thermal conductivity than the base fluid which make a viable heat transfer in fluids. Thermal conductivity is greater in solids than liquids, therefore, the mixture of solids and liquids may settle, clog, foul, erode and cause excessive pressure decrease. Hence, nanotechnology solves these challenges which increase interests in researchers to study nano-particles and heat transfer in fluids. Researchers employ many formulae to determine the thermal conductivity of nano-fluids. Mehrali et al. [47], discussed a comparative study of Nusselt numbers, although the measured thermal conductivities exhibited relatively large deviations from the published correlations. Therefore, changes in thermal conductivity show less severe effects on the modulation of the transport behaviour of nano-fluids [48–50]. For current research work, CMC/water is used as the base fluid (recommendation) having $Pr = 6.2$, to study fluid flow and heat transfer. According to Oztop et al. [51], nano-fluids characteristics are as follows:

$$\alpha_{nf} = \frac{k_{nf}}{(\rho C_p)_{nf}}, \mu_{nf} = \frac{u}{(1 - \varphi)^{2.5}} \frac{k_{nf}}{k_f} = \frac{(k_s + 2k_f) - 2\varphi(k_f - k_s)}{(k_s + 2k_f) + \varphi(k_f + k_s)}, \quad (1)$$

$$(\rho C_p)_{nf} = (1 - \varphi)(\rho C_p)_f + \varphi(\rho C_p)_s, \rho_{nf} = (1 - \varphi)\rho_f + \varphi\rho_s. \quad (2)$$

Water, ethylene glycol, and transformer oil have lower thermal conductivity than nano-structures. Researchers previously reported that the thermal conductivity of nano-fluids was influenced by several parameters. Base fluids type, particle size, particle shape, fluids and temperature are some examples of such parameters [3,49,50,52,53]. Table 1 summarizes the results of thermal conductivity measurement conducted over past 15 years by different research centres.

Table 1. Thermal conductivity of nano-fluids from previous findings.

Researchers	Nano-Particle Size & Shape	Base-Fluids	Observations
Eastman et al. [3]	Cu Spherical	Water	Vol. Fraction 5 to 20%, improvement 10 to 250%.
Murshed et al. [54]	TiO ₂ Spherical (15 nm)	Water	Vol. Fraction 1 to 5%, improvement 18 to 29.7%.
Chen et al. [52]	TiO ₂ Tube shape	Water	Vol. Fraction 0.25 to 0.6%, improvement 2.5 to 4%.
Das et al. [53]	Al ₂ O ₃ Spherical (38.4 nm)	Water	Vol. Fraction 1 to 4%, improvement 2 to 8%.

Effectiveness of Heat Transfer in Nano-Fluids

For nano-fluids used in heat exchange equipment, heat transfer coefficient is superior than thermal conductivity using different nano-particles and base fluids. Therefore, nano-fluids heat transfer has two theories in which the first school of thoughts says that the heat transfer coefficient may be increased without compromising pumping power. The second school of thinking says heat transfer coefficient increases are restricted and mitigated by increased pumping power. MIT and Helmut Schmidt University reflect the second school of thinking. Both groups' findings are in Table 2.

Shriram et al. [55] explored Al₂O₃-water nano-fluids as heat exchanger coolants. Experiments were done at various Reynolds numbers and nano-particle volume concentrations. Therefore, adding nano-particles to the base fluid (CuO-water) increased heat transfer coefficients such that, Khairul et al. [56] tested nano-fluids in a corrugated plate heat exchanger. Water-CuO nano-fluids improved the heat transfer coefficient from 18.50% to 27.20% when nano-particle volume concentration was 0.50% to 1.50%. A Peclet number of about 40,000, Yang et al. [57] evaluated the heat transfer in a circular pipe. Local convective heat transfer improved. Nano-particles and fluid temperature enhanced heat transfer rates. Brownian motion and reduced thermal boundary layer improve heat transfer. Researchers are studying the heat transfer performance of nano-fluids in pipe flow, including natural and induced convection, after Choi et al. [3] reported that nano-sized solid particles boost the thermal conductivity of base fluids.

Table 2. Nano-fluid heat transfer experiment findings.

Researchers	Nano-Particle Size & Shape	Base-Fluids	Observations
Das et al. [53]	Al ₂ O ₃ Spherical (38.4 nm)	Water	Not noticeable rise in <i>Nu</i>
Wen et al. [46]	Al ₂ O ₃ Spherical (30 nm)	Water	Vol. Fraction 0.6 %, <i>Re</i> = 25 to 155, rise in <i>h</i> 1.3 to 12.5 %.
Zeinali et al. [1]	Al ₂ O ₃ Spherical (20 nm)	DI Water	Vol. F. 0.2 to 3.0 %, <i>Re</i> = 650 to 2050, rise in <i>h</i> 10 to 35 %.
Yang et al. [45]	Al ₂ O ₃ Spherical (20 nm to 56 nm)	Water	Vol. F. 0.2 to 1.0 %, <i>Re</i> = 22 to 900, rise in <i>h</i> 3 to 59 %.

2. Mathematical Formulation

Consider the two dimensional and steady state boundary layer (BL) flow over a plate which is flat and permeable. Therefore, the plate is immersed in sodium carboxymethyl cellulose (CMC) nano-fluid, considered as base fluid. The temperature and velocity of

the free stream are denoted by T_∞ and U_∞ . The CMC and water combination, is a non-Newtonian pseudo-plastic fluid. Table 3 has a listing of the viscosity of CMC/water, along with its other features. Experiments show that the thermo-physical properties of CMC/water with a concentration of less than 6% and water with a concentration of 0% are quite similar to one another. Table 4 has a listing of the thermo-physical parameters of the nano-fluids that were taken into consideration. The model takes into consideration a flow regime that is laminar and incompressible. In addition, one of the presumptions is that there is no slippage between the fluid phase and the nano-particles which are in a condition of thermal equilibrium. The continuity, momentum and energy equations constitutes governing system. A magnetic field of strength B_0 that is consistent and applied in a normal direction to the plate. Because it is presumed to be negligible in comparison to the magnetic field that is being applied, the induced magnetic field is ignored.

Table 3. Typical viscosity values for a base fluid (BF) [58].

Physical Characteristics	BF (0%)	BF (0.1%)	BF (0.2%)	BF(0.3%)
n	1	0.91	0.85	0.81
$K/Ns^n m^{-2}$	0.000855	0.006319	0.017540	0.0313603

Table 4. Nano-particles & base fluid thermo-physical characteristics [59].

Physical Characteristics	CMC/Water (0 to 0.3%)	Al_2O_3	TiO_2	Cu	CuO
ρ/kgm^{-3}	997.1	8933	3970	6500	4250
$k/Wm^{-1}K^{-1}$	0.613	400	40	20	8.9538
$C_p/Jkg^{-1}K^{-1}$	4179	385	765	535.6	686.2

In the governing system, the flow velocity is presented by u^* in x and v^* in y directions respectively. The power-law number is indicated by the letter n in the exponent, which is connected to the base fluid. Both Newtonian fluids and pseudo-plastic fluids have n values that are either 1 or between 0 and 1, depending on the kind of fluids. Additionally, the value of n for dilatant fluids is greater than 1. The mass transfer velocity, denoted here by V_w , is something that ought to be thought of as being next to the plate. In the case of an impermeable plate, V_w equals 0. When there is blowing or injection present, V_w has a positive value, but when there is suction present, it has a negative value. The plate becomes heated from the bottom up by a process known as convection, in which a fluid whose temperature is equal to T_f and whose heat transfer coefficient is h_f is responsible for the heating. The governing equations of motion and heat transfer for the classical Blasius and Sakiadis flow of nano-fluids could well be represented using the Boussinesq and boundary layer approximations which are as follows:

Governing Blasius flow:

$$\frac{\partial u^*}{\partial x} + \frac{\partial v^*}{\partial y} = 0, \tag{3}$$

$$u^* \frac{\partial u^*}{\partial x} + v^* \frac{\partial u^*}{\partial y} = \frac{\mu_{nf}}{\rho_{nf}} \frac{\partial}{\partial y} \left(\left| \frac{\partial u^*}{\partial y} \right|^{n-1} \frac{\partial u^*}{\partial y} \right) - \frac{\sigma_{nf} B_0^2}{\rho_{nf}} (u^* - U_\infty), \tag{4}$$

$$u^* \frac{\partial T^*}{\partial x} + v^* \frac{\partial T^*}{\partial y} = \alpha_{nf} \frac{\partial}{\partial y} \left(\left| \frac{\partial T^*}{\partial y} \right|^{n-1} \frac{\partial T^*}{\partial y} \right) + \frac{Q_0}{\rho c_p} (T^* - T_\infty). \tag{5}$$

Boundary conditions for Blasius flow:

$$u^* \rightarrow U_\infty \text{ as } y \rightarrow \infty, u^* = 0, v^* = V_w(x) \text{ as } y = 0. \tag{6}$$

$$-k_{nf} \frac{\partial T^*}{\partial y} = h_f (T_f - T_w) \text{ at } y = 0, T^* \rightarrow T_\infty \text{ as } y \rightarrow \infty. \tag{7}$$

Boundary conditions for Sakiadis flow:

$$u^* \rightarrow U_\infty \text{ as } y \rightarrow \infty, u^* = U_w, v^* = V_W(x) \text{ at } y = 0. \quad (8)$$

$$-k_{nf} \frac{\partial T^*}{\partial y} = h_f(T_f - T_w) \text{ at } y = 0, T^* \rightarrow T_\infty \text{ as } y \rightarrow \infty. \quad (9)$$

Nano-fluids density is represented by ρ_{nf} while the thermal conductivity is scale down under α_{nf} .

3. Solution Methodology

The following similarity transformations have been developed in order to facilitate a more straightforward mathematical analysis of our research:

$$\psi = (U_\infty^{2n-1} v f_x)^{\frac{1}{n+1}} f(\eta), u^* = \frac{\partial \psi}{\partial y}, v^* = -\frac{\partial \psi}{\partial x}, \quad (10)$$

$$\eta = \left(\frac{U_\infty^{2-n}}{v f_x} \right)^{\frac{1}{n+1}} y, \theta = \frac{T^* - T_\infty}{T_f - T_\infty} \quad (11)$$

Therefore, Blasius and Sakiadis' momentum and energy equations with constitutive boundary conditions are;

Governing Blasius flow:

$$\frac{1}{A_4 A_1} (|f''|^{n-1} f'')' + \frac{1}{n+1} f'' f - M^2 \frac{\sigma_{nf}}{\sigma_f} (f' - 1) = 0 \quad (12)$$

$$-\frac{A_3}{Pr_f A_2} (|f''|^{n-1} \theta')' + \frac{1}{n+1} f \theta' \pm \lambda \theta = 0 \quad (13)$$

where

$$\frac{\sigma_{nf}}{\sigma_f} = 1 + \frac{3\varphi \left(\frac{\sigma_s}{\sigma_f} \right) - 1}{\left(\frac{\sigma_s}{\sigma_f} + 2 \right) - \varphi \left(\frac{\sigma_s}{\sigma_f} \right) - 1}, \quad (14)$$

$$M = \sqrt{\left(\frac{x B_0^2}{\rho_{nf}} \right)} \text{ and } \lambda = \frac{Q_0}{\rho C_p}$$

Boundary conditions:

$$f(0) = f_w, f'(0) = 0, f'(\infty) = 1, \quad (15)$$

$$\theta'(0) = A_3 a (1 - \theta(0)), \theta(\infty) = 0. \quad (16)$$

Governing Sakiadis flow:

$$\frac{1}{A_4 A_1} (|f''|^{n-1} f'')' + \frac{1}{n+1} f'' f - M^2 \frac{\sigma_{nf}}{\sigma_f} f' = 0 \quad (17)$$

$$-\frac{A_3}{Pr_f A_2} (|f''|^{n-1} \theta')' + \frac{1}{n+1} f \theta' \pm \lambda \theta = 0 \quad (18)$$

Boundary conditions:

$$f(0) = -f_w, f'(0) = 0, f'(\infty) = 0, \quad (19)$$

$$\theta'(0) = A_3 a (1 - \theta(0)), \theta(\infty) = 0. \quad (20)$$

where $f_w = 0, 1, -1$ stands for impermeable sheet suction and injection respectively.

$$A_1 = \frac{1}{(1 - \varphi) + \frac{\varphi \rho_s}{\rho_f}}, A_2 = -\frac{1}{(1 - \varphi) + \varphi \frac{(\rho C_p)_s}{(\rho C_p)_f}}, \quad (21)$$

$$A_3 = -\frac{\left(\frac{k_s}{k_f} + 2\right) - 2\varphi\left(1 - \frac{k_s}{k_f}\right)}{\left(\frac{k_s}{k_f} + 2\right) + \varphi\left(1 - \frac{k_s}{k_f}\right)}, \quad A_4 = \frac{1}{(1 - \varphi)^{2.5}}. \tag{22}$$

4. Important Engineering Parameters

In this investigation, the local skin friction coefficient C_f and the local Nusselt number Nu_x are considered to be of significant physical consequence, and they can be defined as follows:

$$C_{fx} = -\frac{2\tau_w}{\rho_f U^2}, \quad Nu_x = \frac{xq_w}{k_f(T_w - T_\infty)}, \tag{23}$$

where

$$\tau_w = \mu_{nf} \left(\left| \frac{\partial u^*}{\partial y} \right|^{n-1} \frac{\partial u^*}{\partial y} \right)_{y=0}, \quad q_w = -k_{nf} \left(\frac{\partial T^*}{\partial y} \right)_{y=0}. \tag{24}$$

By employing similarity transformation, the obtained results are as follows:

$$C_{fx} Re_x^{\frac{1}{n+1}} = -2 \frac{\mu_{nf}}{\mu_f} f''(0) |f''(0)|^{n-1}, \tag{25}$$

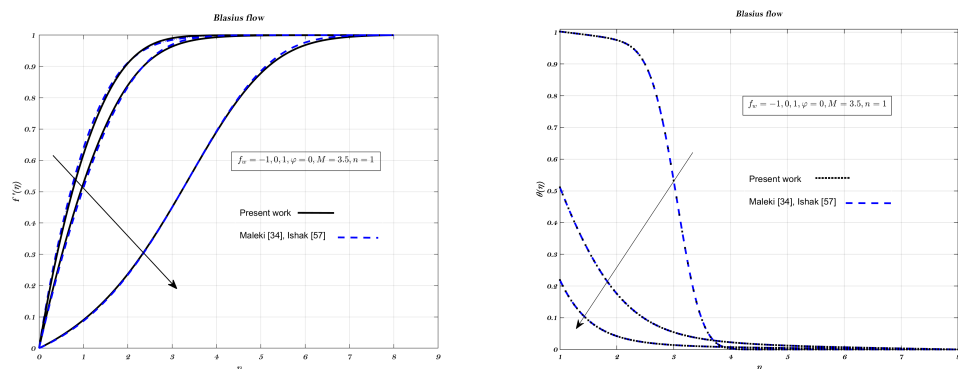
$$Nu_x Re_x^{\frac{-1}{n+1}} = -\frac{k_{nf}}{k_f} \theta'(0).$$

5. Discussion

In this part, the effects of several factors, such as different kind of nano-material, permeability, volume fraction (VF) related to solid particles, index for the power law, magnetic strength, and the source term parameter, has been discussed. For each nano-fluid, the findings are presented with regard to the non-dimensionalized temperature and the velocity fields. The following contains an analysis as well as a discussion of the aforementioned findings.

5.1. Verification

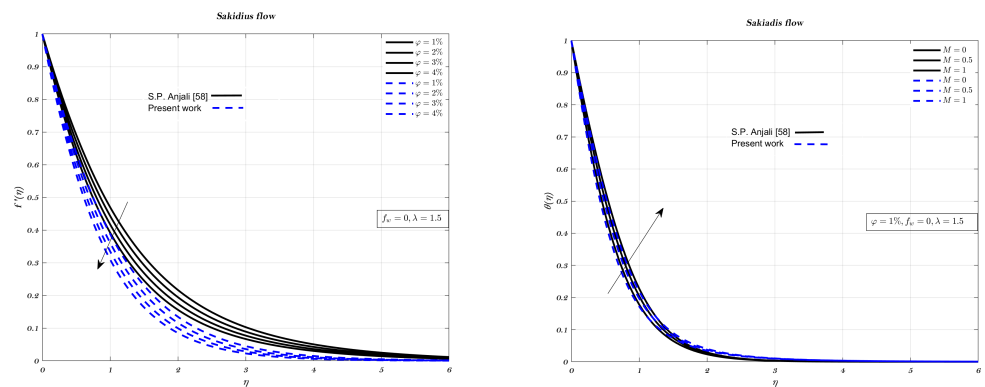
Results from the present experiment are compared and analysed against those from the studies conducted by Maleki and Ishak [32,60], for each combination of φ and f_w . In order to test the correctness of the current numerical work, non-dimensional temperature and velocity profiles give confirmation in case of Blasius flow which can be seen from Figures 1 and 2a,b for Sakiadis flow. It is clear from analysis, that there is a high level of concordance between the old findings [32,60]. It denotes that the existing numerical approach has an excellent accuracy level.



(a) A profile of velocities.

(b) A graph of temperatures.

Figure 1. Impact of different permeability on non-dimensionalized profiles for velocity and temperature.



(a) A profile of velocities.

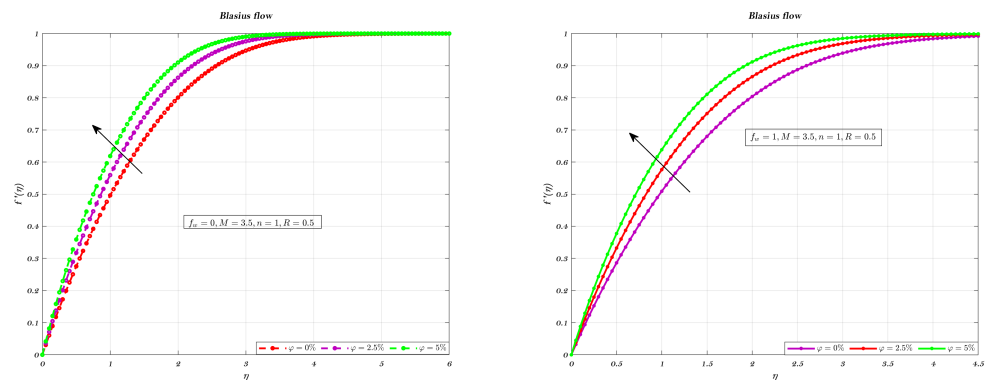
(b) A graph of temperatures.

Figure 2. Impact of different volume fraction on non-dimensionalized velocity and parameter M on temperature profiles.

5.2. The Impact of Investigated Factors on the Flow Velocity Profile

Figures 3a,b and 4a,b illustrate the influence of nano-particles volume fraction for two different values of f_w such as for 0 and 1, which correspond to an impermeable surface and suction, respectively. It has been shown that the fluid velocity increased as the VF which is related to nano particles increased, therefore holds true for both suction and impermeable surfaces [11,31,32,60]. In addition, the employment of Newtonian nano-fluids for suction and an impermeable plate causes a drop in thickness of the boundary layer (BL) but has no effect on the velocity gradient across the plate [32,60].

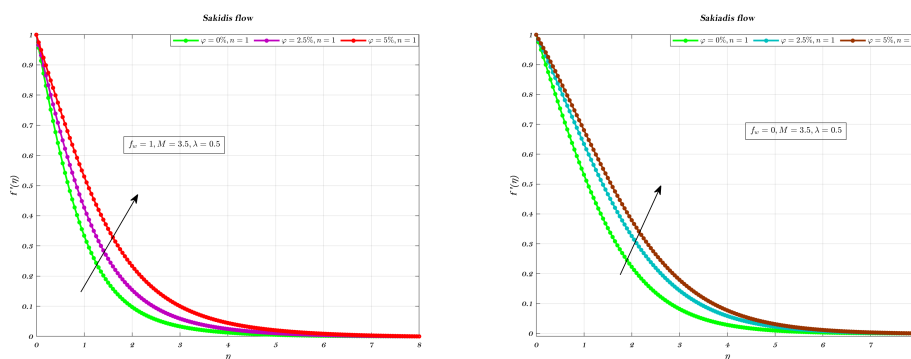
Figure 5a,b illustrate, for both Newtonian and non-Newtonian nano-fluids, the impact of permeability on velocity profile. Because the boundary layer development is regulated by suction, the velocity decreases in proportion to the suction parameter. This is consistent with the fact that suction does stabilise the growth of the boundary layer. Injection, on the other hand, produces greater fluid diffusion and extends the boundary layer. This is shown by the fact that the boundary layer area expands as a result of the injection.



(a) Blasius velocity profile.

(b) Blasius velocity profile.

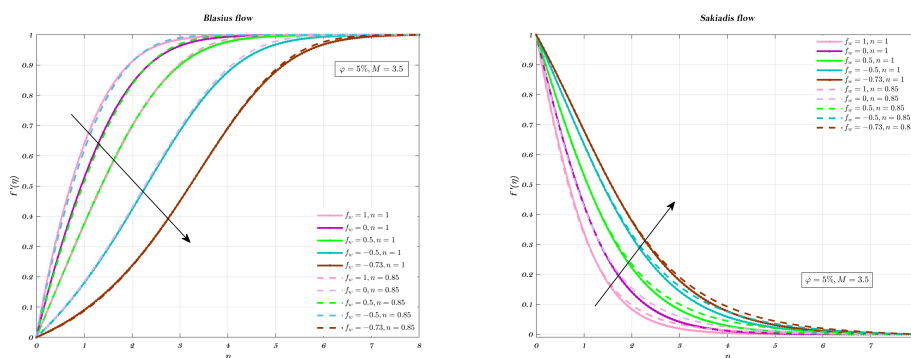
Figure 3. Different VF on non-dimensionalized velocity, by considering $f_w = 0$ & $f_w = 1$.



(a) Sakiadis velocity profile.

(b) Sakiadis velocity profile.

Figure 4. Different VF on non-dimensionalized velocity, by considering $f_w = 1$ & $f_w = 0$.

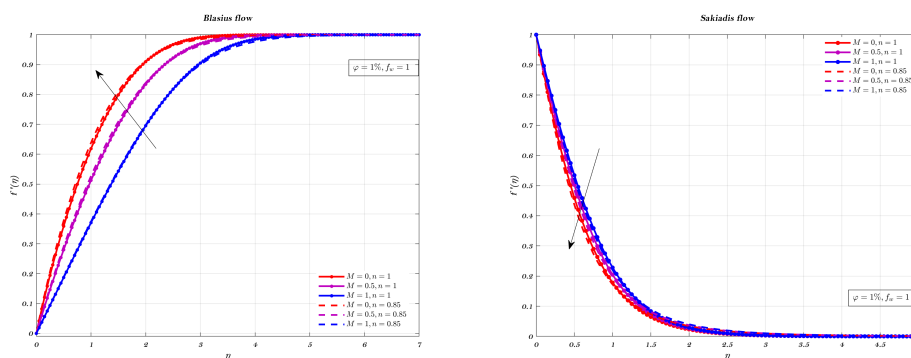


(a) Blasius velocity profile.

(b) Sakiadis velocity profile.

Figure 5. Impact of different permeability, by considering both Newtonian and non-Newtonian cases.

The Blasius flow of Newtonian and non-Newtonian nano-fluids for different values of the magnetic interaction parameter M to analyse non-dimensional velocity, can be seen from Figure 6a. It has been shown without a reasonable doubt that, for both kinds of nano-fluids, the velocity of the nano-fluid rises with an increase in the intensity of the magnetic field. The thickness of the boundary layer will decrease in response to an increase in the intensity of the magnetic field. Therefore, the nano-fluid whose motion is slowed down. Because of this, the velocity of the nano-fluid will rise for both kinds of nano-fluids when the parameter M is increased, the flow will be described as being in a Blasius configuration.



(a) Blasius velocity profile.

(b) Sakiadis velocity profile.

Figure 6. Impact of different values of parameter M on both Newtonian and non-Newtonian cases for Blasius and Sakiadis flows.

Figure 6b illustrates, the magnetic interaction parameter M affects the dimensionless velocity when the Sakiadis flow is considered for both the nano-fluids under consideration. It has been shown that an increase in the magnetic field has the effect of slowing down the velocity. This is due to the fact that the magnetic field in transverse direction generates a resistive force, known as Lorentz force which cut down the hydrodynamic BL thickness for both nano-fluids.

5.3. The Impact of Investigated Factors on the Temperature Profile

Temperature profiles are shown for an impermeable surface, as well as for suction, as seen in the Figures 7 and 8a,b. The decremental status of the dimensionless temperature is because of nano-particles VF in the suction and in the impermeable plate case, however, this decrease is followed by an increase. When an impermeable plate is combined with a non-Newtonian fluid and the addition of nano-particles to increase their volume fraction, results in decrease in temperature. When the plate is subjected to suction, VF does not have significant effects on the surface of the plate. In every instance, the thickness of the BL was reduced when a non-Newtonian fluid is used.

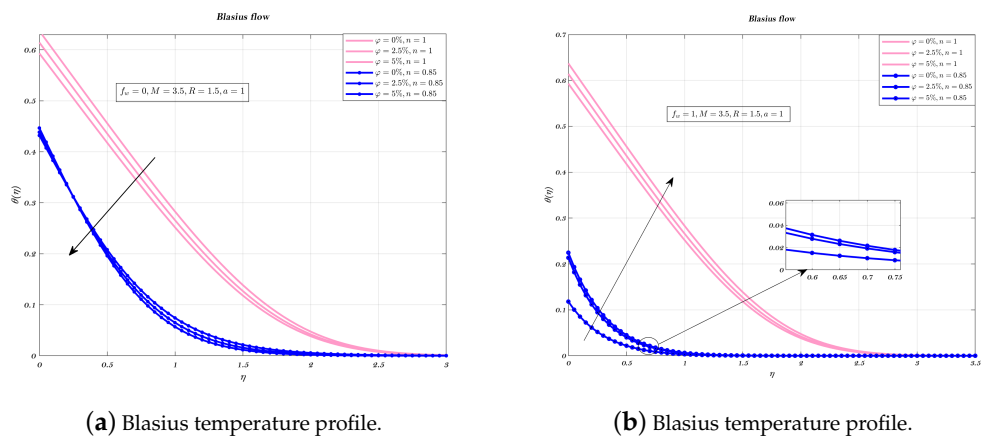


Figure 7. Impact of different volume fraction on non-dimensionalized temperature, by considering $f_w = 0, 1$.

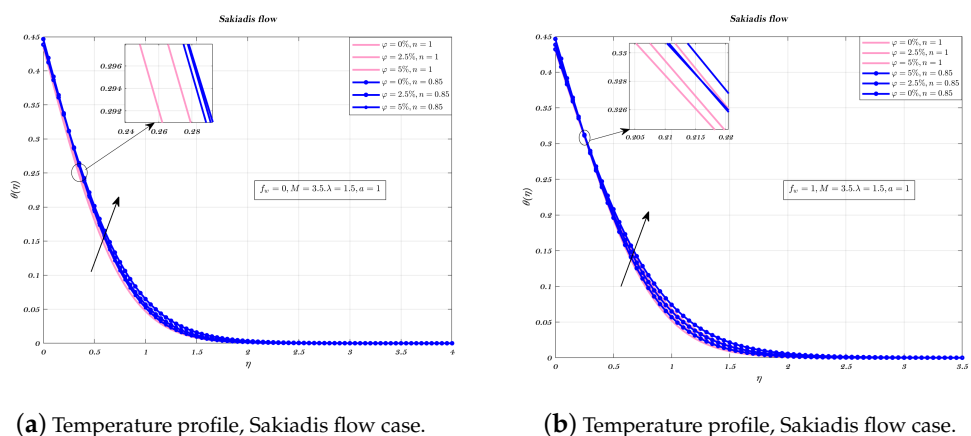


Figure 8. Impact of different volume fraction on non-dimensionalized temperature, by considering $f_w = 0, 1$ for both Newtonian and non-Newtonian cases.

Figures 9–11a,b depict the temperature profile for various values of the index n which is related to the power law for an impermeable surface, suction, and injection. It can be shown that the non-dimensional temperature rises with increasing n for suction and impermeable surface, but this tendency is not apparent for injection. Injection temperatures

do not follow this pattern. Additionally, the thickness of the BL grows in every circumstance as the power-law index rises.

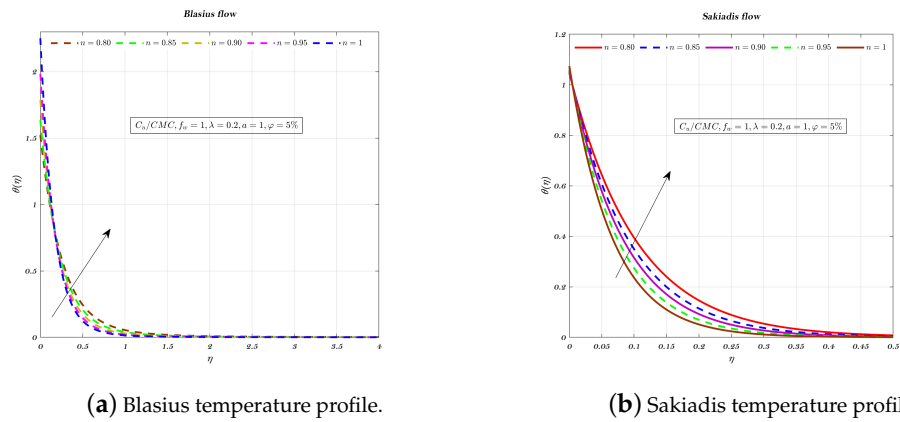


Figure 9. Impact of different values of n on non-dimensionalized temperature, by considering $f_w = 1$ for both flows.

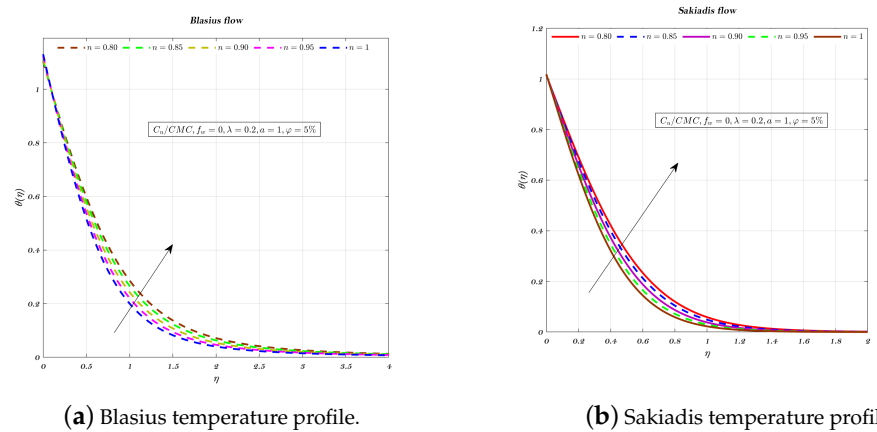


Figure 10. Impact of different values of n on non-dimensionalized temperature, by considering $f_w = 0$ for both flows.

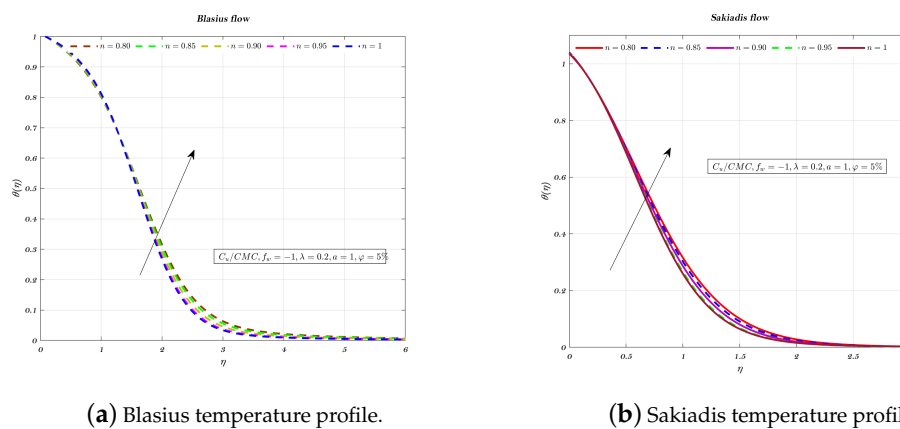


Figure 11. Impact of different values of n on non-dimensionalized temperature, by considering $f_w = -1$ for both flows.

Figure 12a,b depict the influence of a , which is a convective parameter, on temperature profile in which the effect is seen for both types of nano-fluids. As a increases, the surface

temperature $\theta(0)$ also get rise which shows h_f (coefficient of heat transfer) has a relationship that is exactly proportional to the convective parameter. An increase in the convective parameter leads to a decrease in the thermal resistance of the hot surface, which, in turn, causes an increase in the dimensionless surface temperature to be detected. In addition, it is important to notice that as a parameter moves closer and closer to infinity, $\theta(0)$ value moves closer and closer to 1. The injection procedure and the technique for an impermeable surface are identical.

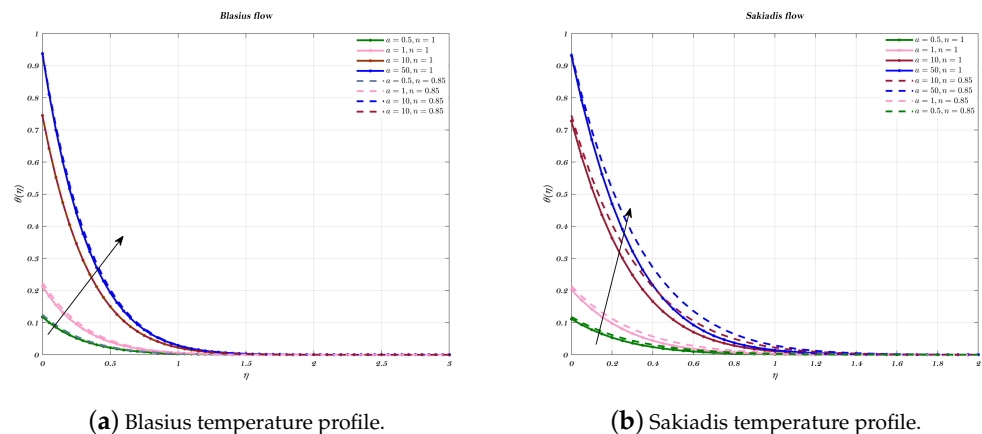


Figure 12. Impact of different values of the convective parameter a on temperature profile, for both flows.

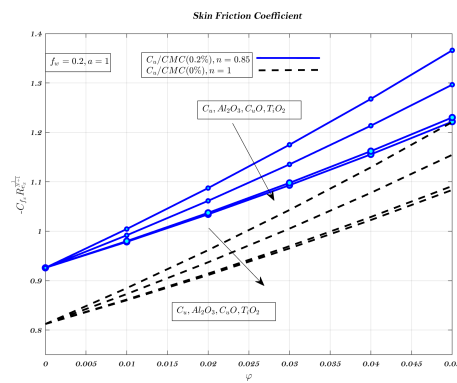
5.4. Variables Affecting Local Nusselt Number and Skin-Friction Coefficient

Different nano-particles have a noticeable effect on the local friction factor for both Newtonian and non-Newtonian nano-fluids, in case of Blasius and Sakiadis flows, as shown in Figure 13a,b. The local friction factor increases when more nano-particles are added to fluids used for transportation. These results highlight the variations in skin friction coefficient over a wide range of VF and magnetic field strengths for both nano-fluids. Therefore, skin friction coefficient founded to increase with both nano-fluids. When the VF of nano-particles is increased, the local friction factor is highest for suction and lowest for injection. Further, the local friction factor of the copper nano-particle is larger than that of other nano-particles. The alumina nano-particle has a lower local friction factor than most other nano-particles. Figures 13–15a indicate that in the case of Blasius flow, non-Newtonian nano-fluids outperform Newtonian nano-fluids in terms of heat transfer efficiency [60].

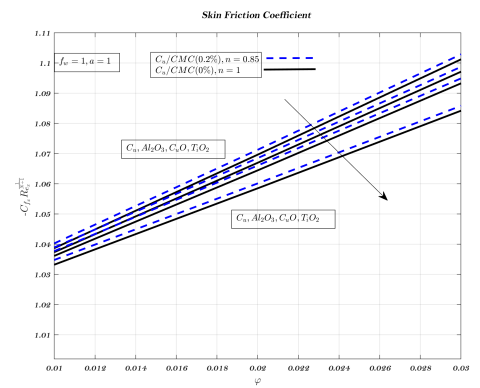
In Sakiadis flow, Figures 13–15b show the influence of VF and parameter related to magnetic field for both nano-fluids on skin friction coefficient. In Sakiadis flow, low-thermal conductivity non-Newtonian nano-fluids have a greater heat transfer rate than Newtonian nano-fluids which is true despite the identical amount of particles in both nano-fluids [5,10,61]. Therefore, with respect to f_w the influence of nano-particle type on heat transfer rate and skin friction is less significant for the impermeable surface, as shown in Figure 14a,b, while its value is lowest for injection, from Figure 15a,b.

Figures 16–18a,b show the impact of nano-particles on impermeable surfaces, suction, and injection. Non-Newtonian fluids increase the Nusselt number when suction and an impermeable surface are present. When injected, non-Newtonian nano-fluids reduce heat transfer. Therefore, mixing the carrying fluid with nano-particles of aluminium oxide or titanium dioxide reduces heat transfer and improves suction. Suction is more favourable for heat transfer than the other two situations in terms of Nusselt number and temperature gradient [32]. Aluminium oxide has greater heat conduction than cupric oxide, but lower heat transfer characteristics [62]. In both kinds of nanofluids, increasing volume fraction and magnetic interaction parameter reduces Nusselt number. Low-thermal conductivity

alumina nano-particles have a greater heat transfer rate than copper nano-particles in Sakiadis flow.

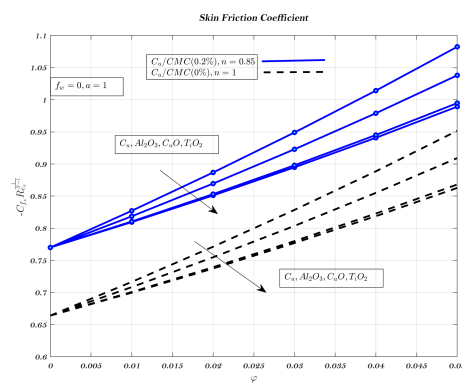


(a) Blasius flow.

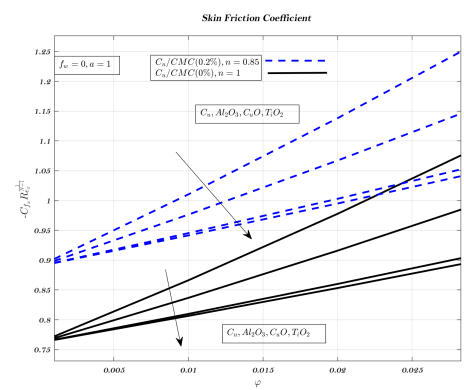


(b) Sakiadis flow.

Figure 13. Impact of different nano-particles on skin friction coefficient by considering $f_w = 0.2$ in case of Blasius flow and $f_w = 1$ for Sakiadis flow.

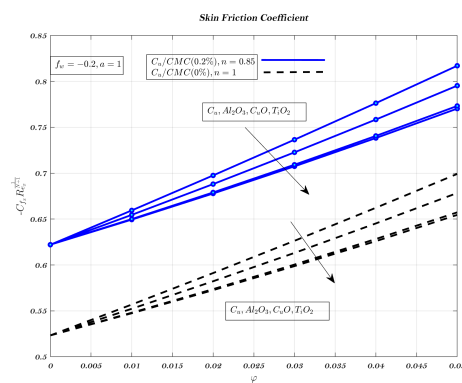


(a) Blasius flow.

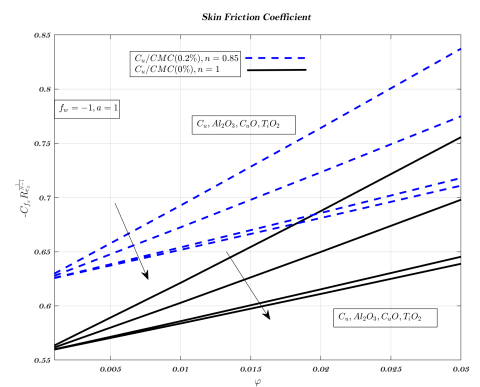


(b) Sakiadis flow.

Figure 14. Impact of different nano-particles on skin friction coefficient by considering $f_w = 0$ in Blasius & Sakiadis flows.



(a) Blasius flow.



(b) Sakiadis flow.

Figure 15. Impact of different nano-particles on skin friction coefficient by considering $f_w = -0.2$ in case of Blasius flow and $f_w = -1$ for Sakiadis flow.

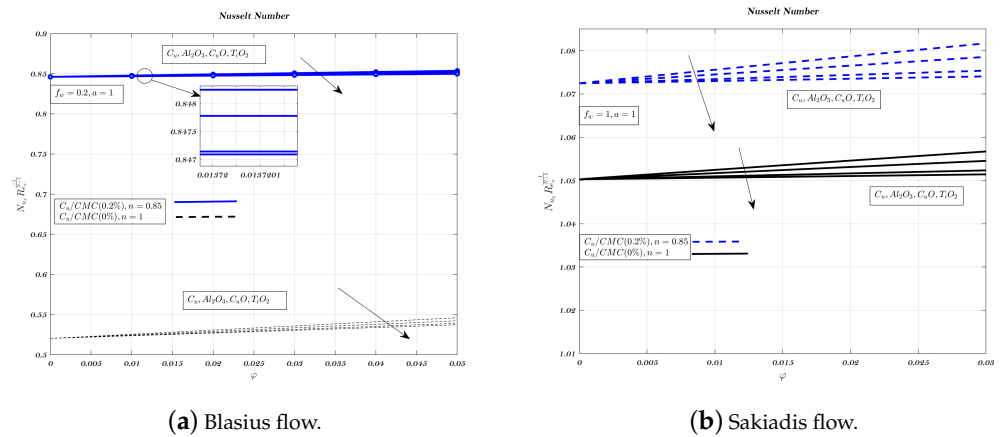


Figure 16. Impact of different nano-particles on Nusselt number by considering $f_w = 0.2$ in case of Blasius flow and $f_w = 1$ for Sakiadis flow.

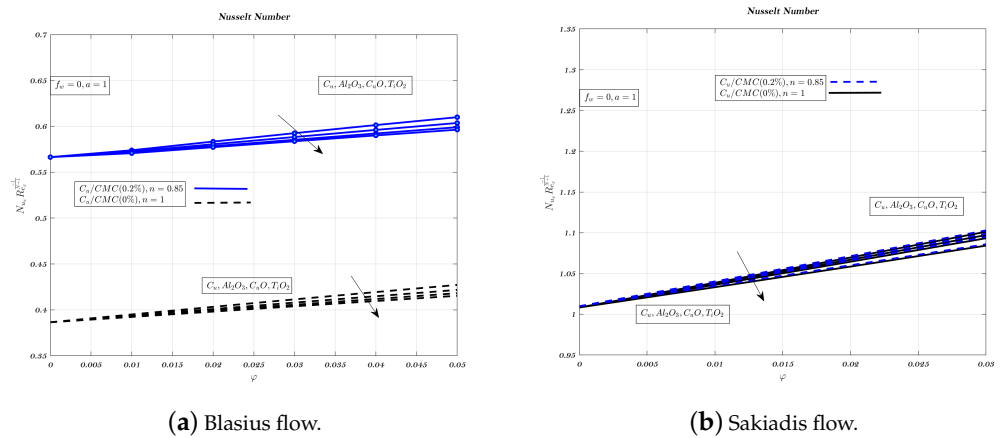


Figure 17. Impact of different nano-particles on Nusselt number by considering $f_w = 0$ in Blasius & Sakiadis flows.

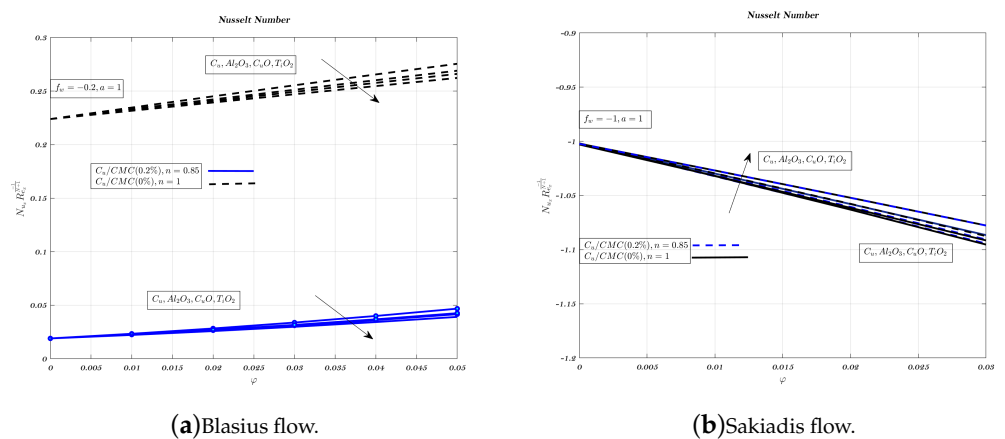


Figure 18. Impact of different nano-particles on Nusselt number by considering $f_w = -0.2$ in case of Blasius flow and $f_w = -1$ for Sakiadis flow.

6. Conclusions

This study examined the boundary layer flow of Newtonian and non-Newtonian nano-fluids across a permeable flat plate in a laminar steady state for Blasius and Sakiadis

flows. The numerical solution to the governing partial differential equations was achieved by translating them to ordinary differential equations (ODEs) using the similarity approach. These ODEs, then numerically solved. Alumina, copper, titanium, and cupric oxide nano-particles were used in the research in which CMC-water served as the base fluid. Some of the study's most significant findings are as follows:

- For suction and impermeable surfaces, nano-particles increase fluid velocity in case of Blasius flow, whereas for injection the tendency is reversed for Sakiadis flow. Also, increasing suction reduced boundary layer thickness.
- Large nano-particle VF reduced plate surface temperature for impermeable surfaces by using fluid which is related to non-Newtonian. For suction, nano-particle volume fraction does not affect the temperature which is on the surface in case of low value of n while it rise up due to parameter related to suction which affects the surface temperature and thermal boundary layer thickness.
- Al_2O_3 has lower heat transfer than CuO despite better heat conduction.
- Nano-particle volume fraction does not always boost heat transfer. In suction, increasing Al_2O_3 and TiO_2 nano-particles reduced heat transfer.
- Non-Newtonian fluid injection reduces heat transfer and increases friction.
- In circumstances that are otherwise identical, the value of the local friction factor is found to be greater for non-Newtonian nano-fluids than it is for Newtonian fluids.
- When compared to other nano-particles, the copper nano-particle has a local friction factor that is much greater but in case of alumina nano-particles, it is much lower.
- The impact of the magnetic field in the Blasius flow is to decrease the temperature while increasing the skin friction coefficient, velocity and reduced Nusselt number for both non-Newtonian & Newtonian nano-fluids. On the other hand, this pattern runs in the opposite direction when Sakiadis flow is considered for either the non-Newtonian & Newtonian nano-fluids.
- In Blasius flow, copper nano-particles enhance nano-fluid velocity, whereas alumina nano-particles have the opposite effect. Sakiadis flow over velocity has the opposite effect. In Blasius flow, increasing φ increases the skin friction coefficient, whereas in Sakiadis flow, both non-Newtonian and Newtonian nano-fluids reverse this tendency.
- Non-Newtonian & Newtonian nano-fluids have greater values for both the skin friction coefficient and the reduced Nusselt number in Blasius flow but for Sakiadis flow, such tendency is inverted.

Author Contributions: Writing—review & editing I.A.; Methodology and Resources S.H. and N.A.A.; Data curation and visualization M.S.; Supervision D.S.M. All authors have read and agreed to the published version of the manuscript.

Funding: This study did not receive any support from any organizations.

Institutional Review Board Statement: Not applicable.

Informed Consent Statement: Not applicable.

Data Availability Statement: Not applicable.

Conflicts of Interest: There is no completing interests, as authors state.

References

1. Zainali, A.; Tofighi, N.; Shadloo, M.S.; Yildiz, M. Numerical investigation of Newtonian and non-Newtonian multiphase flows using ISPH method. *Comput. Methods Appl. Mech. Eng.* **2013**, *254*, 99–113. [[CrossRef](#)]
2. Soltanipour, H.; Choupani, P.; Mirzaee, I. Numerical analysis of heat transfer enhancement with the use of γ - Al_2O_3 /water nanofluid and longitudinal ribs in a curved duct. *Therm. Sci.* **2012**, *16*, 469–480. [[CrossRef](#)]
3. Eastman, J.A.; Choi, S.; Li, S.; Yu, W.; Thompson, L. Anomalously increased effective thermal conductivities of ethylene glycol-based nanofluids containing copper nanoparticles. *Appl. Phys. Lett.* **2001**, *78*, 718–720. [[CrossRef](#)]
4. Dogonchi, A.; Alizadeh, M.; Ganji, D. Investigation of MHD Go-water nanofluid flow and heat transfer in a porous channel in the presence of thermal radiation effect. *Adv. Powder Technol.* **2017**, *28*, 1815–1825. [[CrossRef](#)]

5. Devi, S.; Kandasamy, R. Analysis of nonlinear two dimensional laminar natural flow and mixed convection over variable surface with free stream conditions. *J. Comput. Appl. Math.* **2002**, *3*, 107–116.
6. Ganesh, N.V.; Hakeem, A.A.; Ganga, B. A comparative theoretical study on Al₂O₃ and γ -Al₂O₃ nanoparticles with different base fluids over a stretching sheet. *Adv. Powder Technol.* **2016**, *27*, 436–441. [[CrossRef](#)]
7. Sui, J.; Zheng, L.; Zhang, X.; Chen, G. Mixed convection heat transfer in power law fluids over a moving conveyor along an inclined plate. *Int. J. Heat Mass Transf.* **2015**, *85*, 1023–1033. [[CrossRef](#)]
8. Jalil, M.; Asghar, S. Flow of power-law fluid over a stretching surface: A Lie group analysis. *Int. J. Non-Linear Mech.* **2013**, *48*, 65–71. [[CrossRef](#)]
9. Ahmed, J.; Mahmood, T.; Iqbal, Z.; Shahzad, A.; Ali, R. Axisymmetric flow and heat transfer over an unsteady stretching sheet in power law fluid. *J. Mol. Liq.* **2016**, *221*, 386–393. [[CrossRef](#)]
10. Guha, A.; Pradhan, K. Natural convection of non-Newtonian power-law fluids on a horizontal plate. *Int. J. Heat Mass Transf.* **2014**, *70*, 930–938. [[CrossRef](#)]
11. Megahed, A.M. Flow and heat transfer of a non-Newtonian power-law fluid over a non-linearly stretching vertical surface with heat flux and thermal radiation. *Meccanica* **2015**, *50*, 1693–1700. [[CrossRef](#)]
12. Saritha, K.; Rajasekhar, M.; Reddy, B.S. Heat and mass transfer of laminar boundary layer flow of non-Newtonian power law fluid past a porous flat plate with Soret and Dufour effects. *Phys. Sci. Int. J.* **2016**, *11*, 1–13. [[CrossRef](#)]
13. Rajput, G.R.; Prasad, J.K.; Timol, M. Similarity flow solution of MHD boundary layer model for non-Newtonian power-law fluids over a continuous moving surface. *Gen* **2014**, *24*, 97–102.
14. Naikoti, K.; Borra, S.R. Quasi-linearization approach to MHD effects on boundary layer flow of power-law fluids past a semi infinite flat plate with thermal dispersion. *Int. J. Non-Linear Sci.* **2011**, *11*, 301–311.
15. RamReddy, C.; Naveen, P.; Srinivasacharya, D. nonlinear convective flow of non-Newtonian fluid over an inclined plate with convective surface condition: A Darcy–Forchheimer model. *Int. J. Appl. Comput. Math.* **2018**, *4*, 1–18. [[CrossRef](#)]
16. Mahmoud, M.A. Slip velocity effect on a non-Newtonian power-law fluid over a moving permeable surface with heat generation. *Math. Comput. Model.* **2011**, *54*, 1228–1237. [[CrossRef](#)]
17. Li, B.; Zheng, L.; Zhang, X. Heat transfer in pseudo-plastic non-Newtonian fluids with variable thermal conductivity. *Energy Convers. Manag.* **2011**, *52*, 355–358. [[CrossRef](#)]
18. Yazdi, M.; Hashim, I.; Sopian, K. Slip boundary layer flow of a power-law fluid over moving permeable surface with viscous dissipation and prescribed surface temperature. *Int. Rev. Mech. Eng.* **2014**, *8*, 661–670.
19. Si, X.; Li, H.; Shen, Y.; Zheng, L. Effects of nonlinear velocity slip and temperature jump on pseudo-plastic power-law fluid over moving permeable surface in presence of magnetic field. *Appl. Math. Mech.* **2017**, *38*, 333–342. [[CrossRef](#)]
20. Shamshirband, S.; Malvandi, A.; Karimipour, A.; Goodarzi, M.; Afrand, M.; Petković, D.; Dahari, M.; Mahmoodian, N. Performance investigation of micro-and nano-sized particle erosion in a 90 elbow using an ANFIS model. *Powder Technol.* **2015**, *284*, 336–343. [[CrossRef](#)]
21. Hajmohammadi, M.; Maleki, H.; Lorenzini, G.; Nourazar, S. Effects of Cu and Ag nano-particles on flow and heat transfer from permeable surfaces. *Adv. Powder Technol.* **2015**, *26*, 193–199. [[CrossRef](#)]
22. Akbari, O.A.; Toghraie, D.; Karimipour, A.; Safaei, M.R.; Goodarzi, M.; Alipour, H.; Dahari, M. Investigation of rib's height effect on heat transfer and flow parameters of laminar water–Al₂O₃ nanofluid in a rib-microchannel. *Appl. Math. Comput.* **2016**, *290*, 135–153.
23. Heydari, A.; Akbari, O.A.; Safaei, M.R.; Derakhshani, M.; Alrashed, A.A.; Mashayekhi, R.; Ahmadi Sheikh Shabani, G.; Zarringhalam, M.; Nguyen, T.K. The effect of attack angle of triangular ribs on heat transfer of nanofluids in a microchannel. *J. Therm. Anal. Calorim.* **2018**, *131*, 2893–2912. [[CrossRef](#)]
24. Afrand, M.; Nadooshan, A.A.; Hassani, M.; Yarmand, H.; Dahari, M. Predicting the viscosity of multi-walled carbon nanotubes/water nanofluid by developing an optimal artificial neural network based on experimental data. *Int. Commun. Heat Mass Transf.* **2016**, *77*, 49–53. [[CrossRef](#)]
25. Sarsam, W.S.; Amiri, A.; Shanbedi, M.; Kazi, S.; Badarudin, A.; Yarmand, H.; Bashirnezhad, K.; Zaharinie, T. Synthesis, stability, and thermophysical properties of aqueous colloidal dispersions of multi-walled carbon nanotubes treated with beta-alanine. *Int. Commun. Heat Mass Transf.* **2017**, *89*, 7–17. [[CrossRef](#)]
26. Safaei, M.R.; Safdari Shadloo, M.; Goodarzi, M.S.; Hadjadj, A.; Goshayeshi, H.R.; Afrand, M.; Kazi, S. A survey on experimental and numerical studies of convection heat transfer of nanofluids inside closed conduits. *Adv. Mech. Eng.* **2016**, *8*, 1687814016673569. [[CrossRef](#)]
27. Hosseini, S.M.; Safaei, M.R.; Goodarzi, M.; Alrashed, A.A.; Nguyen, T.K. New temperature, interfacial shell dependent dimensionless model for thermal conductivity of nanofluids. *Int. J. Heat Mass Transf.* **2017**, *114*, 207–210. [[CrossRef](#)]
28. Nandeppanavar, M.M.; Reddy Gorla, R.S.; Shakunthala, S. Magneto-hydrodynamic Blasius flow and heat transfer from a flat plate in the presence of suspended carbon nanofluids. *Proc. Inst. Mech. Eng. Part J. Nanomater. Nanoeng. Nanosyst.* **2018**, *232*, 31–40. [[CrossRef](#)]
29. Lin, Y.; Zheng, L.; Zhang, X. Radiation effects on Marangoni convection flow and heat transfer in pseudo-plastic non-Newtonian nanofluids with variable thermal conductivity. *Int. J. Heat Mass Transf.* **2014**, *77*, 708–716. [[CrossRef](#)]
30. Ramesh, G.; Chamkha, A.J.; Gireesha, B. Magnetohydrodynamic flow of a non-Newtonian nanofluid over an impermeable surface with heat generation/absorption. *J. Nanofluids* **2014**, *3*, 78–84. [[CrossRef](#)]

31. Uddin, M.; Ferdows, M.; Bég, O.A. Group analysis and numerical computation of magneto-convective non-Newtonian nanofluid slip flow from a permeable stretching sheet. *Appl. Nanosci.* **2014**, *4*, 897–910. [[CrossRef](#)]
32. Maleki, H.; Safaei, M.R.; Alrashed, A.A.; Kasaeian, A. Flow and heat transfer in non-Newtonian nanofluids over porous surfaces. *J. Therm. Anal. Calorim.* **2019**, *135*, 1655–1666. [[CrossRef](#)]
33. Jamaludin, A.; Naganthran, K.; Nazar, R.; Pop, I. Thermal radiation and MHD effects in the mixed convection flow of Fe₃O₄–water ferrofluid towards a nonlinearly moving surface. *Processes* **2020**, *8*, 95. [[CrossRef](#)]
34. Jamaludin, A.; Naganthran, K.; Nazar, R.; Pop, I. MHD mixed convection stagnation-point flow of Cu–Al₂O₃/water hybrid nanofluid over a permeable stretching/shrinking surface with heat source/sink. *Eur. J. -Mech.-B/Fluids* **2020**, *84*, 71–80. [[CrossRef](#)]
35. Hamilton, R.L.; Crosser, O. Thermal conductivity of heterogeneous two-component systems. *Ind. Eng. Chem. Fundam.* **1962**, *1*, 187–191. [[CrossRef](#)]
36. Sandeep, N.; Kumar, B.R.; Kumar, M.J. A comparative study of convective heat and mass transfer in non-Newtonian nanofluid flow past a permeable stretching sheet. *J. Mol. Liq.* **2015**, *212*, 585–591. [[CrossRef](#)]
37. Madhu, M.; Kishan, N.; Chamkha, A. Boundary layer flow and heat transfer of a non-Newtonian nanofluid over a non-linearly stretching sheet. *Int. J. Numer. Methods Heat Fluid Flow* **2016**, *26*, 2198–2217. [[CrossRef](#)]
38. Chen, C.H. Effects of magnetic field and suction/injection on convection heat transfer of non-Newtonian power-law fluids past a power-law stretched sheet with surface heat flux. *Int. J. Therm. Sci.* **2008**, *47*, 954–961. [[CrossRef](#)]
39. Kumar, R.; Sood, S.; Shehzad, S.A.; Sheikholeslami, M. Radiative heat transfer study for flow of non-Newtonian nanofluid past a Riga plate with variable thickness. *J. Mol. Liq.* **2017**, *248*, 143–152. [[CrossRef](#)]
40. Saranya, S.; Al-Mdallal, Q.M. Non-Newtonian ferrofluid flow over an unsteady contracting cylinder under the influence of aligned magnetic field. *Case Stud. Therm. Eng.* **2020**, *21*, 100679. [[CrossRef](#)]
41. Sarada, K.; Gowda, R.J.P.; Sarris, I.E.; Kumar, R.N.; Prasannakumara, B.C. Effect of magnetohydrodynamics on heat transfer behaviour of a non-Newtonian fluid flow over a stretching sheet under local thermal non-equilibrium condition. *Fluids* **2021**, *6*, 264. [[CrossRef](#)]
42. Ishtiaq, F.; Ellahi, R.; Bhatti, M.M.; Alamri, S.Z. Insight in thermally radiative cilia-driven flow of electrically conducting non-newtonian jeffrey fluid under the influence of induced magnetic field. *Mathematics* **2022**, *10*, 2007. [[CrossRef](#)]
43. Abderrahmane, A.; Alqsair, U.F.; Guedri, K.; Jamshed, W.; Nasir, N.A.A.; Majdi, H.S.; Baghaei, S.; Mourad, A.; Marzouki, R. Analysis of mixed convection of a power-law non-Newtonian nanofluid through a vented enclosure with rotating cylinder under magnetic field. *Ann. Nucl. Energy* **2022**, *178*, 109339. [[CrossRef](#)]
44. Levin, M.L.; Miller, M.A. Maxwell's "Treatise on Electricity and Magnetism". *Sov. Phys. Uspekhi* **1981**, *24*, 904. [[CrossRef](#)]
45. Yang, Y. *Characterizations and Convective Heat Transfer Performance of Nanofluids*; Lehigh University: Bethlehem, PA, USA, 2011.
46. Wen, D.; Ding, Y. Effective thermal conductivity of aqueous suspensions of carbon nanotubes (carbon nanotube nanofluids). *J. Thermophys. Heat Transf.* **2004**, *18*, 481–485. [[CrossRef](#)]
47. Mehrali, M.; Sadeghinezhad, E.; Latibari, S.T.; Kazi, S.N.; Mehrali, M.; Zubir, M.N.B.M.; Metselaar, H.S.C. Investigation of thermal conductivity and rheological properties of nanofluids containing graphene nanoplatelets. *Nanoscale Res. Lett.* **2014**, *9*, 1–12. [[CrossRef](#)]
48. Koblinski, P.; Phillpot, S.; Choi, S.; Eastman, J. Mechanisms of heat flow in suspensions of nano-sized particles (nanofluids). *Int. J. Heat Mass Transf.* **2002**, *45*, 855–863. [[CrossRef](#)]
49. Duangthongsuk, W.; Wongwises, S. Comparison of the effects of measured and computed thermophysical properties of nanofluids on heat transfer performance. *Exp. Therm. Fluid Sci.* **2010**, *34*, 616–624. [[CrossRef](#)]
50. Yu, W.; Choi, S. The role of interfacial layers in the enhanced thermal conductivity of nanofluids: A renovated Maxwell model. *J. Nanoparticle Res.* **2003**, *5*, 167–171. [[CrossRef](#)]
51. Öziş, T.; Aslan, İ. Similarity solutions to Burgers' equation in terms of special functions of mathematical physics. *Acta Phys. Pol. B* **2017**, *48*, 1349–1366. [[CrossRef](#)]
52. Chen, H.; Yang, W.; He, Y.; Ding, Y.; Zhang, L.; Tan, C.; Lapkin, A.A.; Bavykin, D.V. Heat transfer and flow behaviour of aqueous suspensions of titanate nanotubes (nanofluids). *Powder Technol.* **2008**, *183*, 63–72. [[CrossRef](#)]
53. Das, S.K.; Putra, N.; Thiesen, P.; Roetzel, W. Temperature dependence of thermal conductivity enhancement for nanofluids. *J. Heat Transf.* **2003**, *125*, 567–574. [[CrossRef](#)]
54. Murshed, S.; Leong, K.; Yang, C. Enhanced thermal conductivity of TiO₂–Water based nanofluids. *Int. J. Therm. Sci.* **2005**, *44*, 367–373. [[CrossRef](#)]
55. Sonawane, S.S.; Khedkar, R.S.; Wasewar, K.L. Study on concentric tube heat exchanger heat transfer performance using Al₂O₃–Water based nanofluids. *Int. Commun. Heat Mass Transf.* **2013**, *49*, 60–68. [[CrossRef](#)]
56. Khairul, M.A.; Alim, M.A.; Mahbulul, I.M.; Saidur, R.; Hepbasli, A.; Hossain, A. Heat transfer performance and exergy analyses of a corrugated plate heat exchanger using metal oxide nanofluids. *Int. Commun. Heat Mass Transf.* **2014**, *50*, 8–14. [[CrossRef](#)]
57. Yang, J.; Li, F.; Xu, H.; He, Y.; Huang, Y.; Jiang, B. Heat transfer performance of viscoelastic-fluid-based nanofluid pipe flow at entrance region. *Exp. Heat Transf.* **2015**, *28*, 125–138. [[CrossRef](#)]
58. Zhang, H.; Zhang, X.; Zheng, L. Numerical study of thermal boundary layer on a continuous moving surface in power law fluids. *J. Therm. Sci.* **2007**, *16*, 243–247. [[CrossRef](#)]
59. Abu-Nada, E. Application of nanofluids for heat transfer enhancement of separated flows encountered in a backward facing step. *Int. J. Heat Fluid Flow* **2008**, *29*, 242–249. [[CrossRef](#)]

60. Ishak, A. Similarity solutions for flow and heat transfer over a permeable surface with convective boundary condition. *Appl. Math. Comput.* **2010**, *217*, 837–842. [[CrossRef](#)]
61. Anjali Devi, S.; Suriyakumar, P. Effect of magnetic field on Blasius and Sakiadis flow of nanofluids past an inclined plate. *J. Taibah Univ. Sci.* **2017**, *11*, 1275–1288. [[CrossRef](#)]
62. Tiwari, R.K.; Das, M.K. Heat transfer augmentation in a two-sided lid-driven differentially heated square cavity utilizing nanofluids. *Int. J. Heat Mass Transf.* **2007**, *50*, 2002–2018. [[CrossRef](#)]